Regular Article

Solution Equilibrium Study of Divalent Metal Ions with Phenylpropanoid Derivatives and Acetylcysteine Ligands

Thuy Thi Dieu Nguyen,[a,#] Shella Permatasari Santoso,[a,#] Thuyen Thi Bich Nguyen,[a] Artik Elisa Angkawijaya,[a,b] Phuong Lan Tran-Nguyen,[c] and Yi Hsu Ju*,[a]

[a] *Department of Chemical Engineering, National Taiwan University of Science and Technology; Taipei 106–07, Taiwan, R. O. C.:* [b] *Institute of Plant and Microbial Biology, Academia Sinica; Taipei 115–29, Taiwan, R.O.C.: and* [c] *Department of Mechanical Engineering, Can Tho University; 3–2 Street, Cantho City, Viet Nam.*
Received May 5, 2016; accepted July 28, 2016

Solution equilibrium of divalent metal ions (M=Mn^{2+}, Co^{2+}, Ni^{2+}, Cu^{2+} and Zn^{2+}) with caffeic acid (ligand C) or dihydrocaffeic acid (ligand D) in binary system, and with acetylcysteine (ligand N) in ternary system were investigated at condition similar to human physiological temperature of 310.15 K and ionic strength of 0.15 mol·dm^{-3} NaCl. Potentiometry technique was used for the determination of formation constant (logβ) assisted by spectrophotometry technique. The results indicated the formation of [ML], [MLH], [ML_2], [ML_2H] in binary species and [MLN], [MNLH], [$MNLH_2$] in ternary species, where L represents ligands C or D. It was found that ligand D formed more stable complexes than that of ligand C, which were affected by the presence of double bond in the carboxylate moiety of ligand C. The speciation diagrams were simulated by HySS and discussed briefly, additionally the tendency of ternary complexes was evaluated from parameters $\Delta \log K_M$ and $\log X$.

Key words solution equilibrium; phenylpropanoid complex; caffeic acid; dihydrocaffeic acid; metal complex; acetylcysteine

Metal elements have been known capable of causing severe health problems for human.[1)] Redox-inert metals such as mercury (Hg), lead (Pb) and cadmium (Cd) are toxic agents, exposure to these and other essential metals may cause negative effects on health.[2)] Metals are known to be able to bind with proteins in human body which may lead to various detrimental effects on human health. For instance, high exposure of zinc results in respiratory and gastrointestinal toxicity, clinical changes and copper deficiency.[3)] Excess amount of copper can cause serious diseases including cancers, liver and kidney damage.[4)] Cobalt exposure leads to ailment such as vision problem, lung problem, heart problem and thyroid damage. Exposure to manganese can cause disorders such as Parkinson, schizophrenia and dullness. Although nickel appears to be essential for plants and bacteria, however for human this metal was found to be difficult to elucidate and may cause severe health problems such as cancer.[5)]

Chelation therapy is known as an effective treatment to reduce the harmful effects of metal ions by utilizing the metal binding ability of organic ligand.[6–10)] Therefore to prevent metal intoxication, the ligand used should have stronger binding ability than the proteins. Phenylpropanoid derivatives, currently considered as promising chelating agents, are classified as phenolic acids that are known to function as natural antioxidant, free radical scavenger, anti-carcinogenic, and chemoprevention agent.[11–14)] In this work, caffeic acid and dihydrocaffeic acid were chosen as the phenylpropanoid derivatives. Caffeic acid (denoted as ligand C) is an important anti-oxidative compound which can be extracted from natural sources such as coffee bean, potatoes, grains and vegetables.[15)] This compound has beneficial pharmacological effects such as inhibit cancer cell in human HT-1080 fibro sarcoma cell line.[16,17)] Dihydrocaffeic acid (denoted as ligand D) is a degradation product of caffeic acid, this compound is one of the critical phenolic antioxidants commonly present in olives,[18)] and in blood or urine as the result of secondary metabolism of various polyphenols.[19)] The *ortho*-dihydroxyl structure of ligand D is also known to act as an active radical-scavenger.[15)]

On the other hand, acetylcysteine is an organic compound which has been approved as one of the essential medicines for basic health system by World Health Organization (WHO).[20)] Acetylcysteine is known as a precursor for glutathione, the antioxidant which prevents formation of oxidative species in tissue.[21,22)] Thiol group of acetylcysteine can prevent sulfur depletion in body.[23)] This compound also has been reported as a potential chelating agent for some metals such as Mn^{2+}, Ni^{2+}, Co^{2+}, Zn^{2+}, Cu^{2+}, Cd^{2+} and Hg^{2+}.[22,24,25)] The mixed ligand combination of acetylcysteine and ligands C or D is expected to improve the stability of the chelate complex.

Recently, the complexation of ligands C and D with metal ion has gained attention of some researchers.[26–30)] To the best of our knowledge, very few literatures are available for the complexation study of ligand D with essential divalent metal ions. Therefore, in order to gain primary understanding on the complexation of ligands C and D, potentiometry technique was conducted (at T=310.15 K and ionic strength I=0.15 mol·dm^{-3} NaCl) to investigate the complexation ability of the ligands against divalent metal ions (Mn^{2+}, Co^{2+}, Ni^{2+}, Cu^{2+}, Zn^{2+}). The specific temperature and ionic strength were chosen to provide an environment similar to typical physiological condition for human. In this study, the contribution of double bond on carboxylate side chain of ligand C in the formation of complex was also evaluated. The study was conducted in binary system and in ternary system (with acetylcysteine, denoted as ligand N). In addition, UV-Vis spectrophotometry measurement was also performed to study the protonation constants of

[#] These authors contributed equally to this work.

* To whom correspondence should be addressed. e-mail: yhju@mail.ntust.edu.tw

ligands C and D and to confirm the stability constant values.

Experimental

Materials and Solution Analytical grade ligands, dihydrocaffeic acid ($C_9H_{10}O_4$, 98% purity) purchased from Alfa Aesar (Lancashire, U.K.), caffeic acid ($C_9H_8O_4$, 99% purity) and acetylcysteine ($C_5H_9NO_3S$, 99% purity) provided by Sigma-Aldrich (Steinheim, Germany), were directly used without further purification. Divalent metal salts were standardized against ethylenediaminetetraacetic acid (EDTA), their suppliers are as follows: zinc nitrate hexahydrate ($Zn(NO_3)_2\cdot 6H_2O$, 98% purity)—Acros Organics (Morris Plains, NJ, U.S.A.), nickel chloride hexahydrate ($NiCl_2\cdot 6H_2O$, 98% purity)—Alfa Aesar (Lancashire, U.K.), dihydrate cupric chloride salt ($CuCl_2\cdot 2H_2O$, 99% purity) and cobalt nitrate hexahydrate ($Co(NO_3)_2\cdot 6H_2O$, 98% purity)—Sigma-Aldrich (Steinheim, Germany), manganese chloride tetrahydrate ($MnCl_2\cdot 4H_2O$, 99.8% purity)—Fisher Scientific (Hampton, NH, U.S.A.).

Prior to acidify the solutions, hydrochloric acid (HCl, 36.5%, Acros Organics) were prepared and standardized before used. As the titrant, carbonate-free sodium hydroxide (NaOH, 96% purity, Yakuri Pure Chemicals, Kyoto, Japan) was prepared and standardized with potassium hydrogen phthalate (KHP, 99.85% purity, Sigma-Aldrich). The ionic strength was maintained constant by using sodium chloride (NaCl, 99.5% purity, Showa, Tokyo, Japan). All stock solutions were freshly prepared in deionized (DI) water (>18.3 $M\Omega\cdot cm^{-1}$ resistance).

Potentiometry Measurement Potentiometry measurement was carried out using a Metrohm 888-Titrando Dosimat model 805, supported with an 802-rod stirrer, an 804 Ti stand and coupled with a combined Ecotrode Plus pH-glass electrode (4 decimals readability). The apparatus was connected to a personal computer and monitored by Tiamo 2.3 computer software. All experiments were carried out in a 150 cm^3 double walled glass reactor. All measurements were done in triplicate. Carbonate-free NaOH (0.1 $mol\cdot dm^{-3}$) was used as the titrant against these following solutions:

(a) 3×10^{-3} $mol\cdot dm^{-3}$ HCl+1.5×10^{-2} $mol\cdot dm^{-3}$ NaCl.
(b) Solution (a)+0.01 $mol\cdot dm^{-3}$ ligands C or D.
(c) Solution (a)+(0.01–0.012) $mol\cdot dm^{-3}$ ligands C or D+(0.004–0.01) $mol\cdot dm^{-3}$ metal salt. The metal to ligand concentration ratios used are 1 : 1, 1 : 2, 1 : 2.5 and 1 : 3.
(d) Solution (a)+0.01 $mol\cdot dm^{-3}$ C or 0.01 $mol\cdot dm^{-3}$ D+0.01 $mol\cdot dm^{-3}$ ligand N+0.01 $mol\cdot dm^{-3}$ metal salt, with metal to ligands ratio of 1 : 1 : 1.

Since the potentiometry method involves the titration of strong acid and strong base therefore it was necessary to perform the electrode calibration in terms of hydrogen ion concentration by using the program GLEE. This program not only provides the electrode calibration constants but also the estimation of the carbonate contamination of the base. The potentiometry titrations were performed at T=310.15 K and I=0.15 $mol\cdot dm^{-3}$ NaCl, in this condition the self-dissociation constant of water is pK_w=13.384.

Spectrophotometry Measurement UV-Vis spectrophotometer Jasco V-550 was used to collect the spectrum data of ligands in the absence and presence of metal ions at the wavelength range of 200 to 800 nm. The instrument uses a deuterium lamp at higher energies and halogen lamp at lower energies. The measured solution was put in a standard 10 mm standard quartz cell. The concentration of the solutions used was one tenth of that used in potentiometry measurement.

Data Analysis Hyperquad2008 was selected among several non-linear-square algorithm computer programs because of its simplicity and accuracy in determining the equilibrium constant,[31] especially when several equilibrium reactions take place in the analyzed solution. The results of an equilibrium constant refinement may contain various pieces of information such as:

a. The Overall Formation Constant (β_{pqrs})

$$pM+qN+rL+sH \rightleftharpoons M_pN_qL_rH_s,\quad [M_pN_qL_rH_s]=\beta_{pqrs}[M]^p[N]^q[L]^r[H]^s \tag{1}$$

where the stoichiometry coefficient p, q, r, s refer to metal ion, ligand N, ligands C or D and hydrogen atom, respectively.

b. Standard Deviations

Standard deviation is obtained by an error-propagation calculation from experimental errors, where the confident limit is ≤0.1.

c. Goodness of Fitting (σ)

The σ value is obtained from the Eq. 2:

$$\sigma=\sqrt{\frac{\sum_{i=1,np}(W_i r_i^2)}{(m-n)}} \tag{2}$$

where W_i, r_i, m, n refer to the weight at the i-th data point, the residual at the i-th data point, the number of titration data points and the number of refined parameters, respectively. The σ value range is 1.17–1.35, which specifically represents 95% goodness of fitting.

The spectrophotometry data were analyzed by using the Hypspec[32] and the speciation diagrams were simulated by the HySS program.[33]

Structure Modeling Gaussian09W program with density functional theory (DFT), B3LYP and 6–31+G(d) basis set was used for the calculation of Gibb's free energy. Structure optimization and frequency analysis were applied prior to obtaining the thermochemical properties of the complex species.

Results and Discussion

Protonation Constants Both ligand C and ligand D are tri-protic ligands with three functional groups *viz.* carboxylic group, *meta*- and *para*-hydroxyl groups. The protonation constants of the ligands are presented in Table 1 as minus logarithm of a protonation constant or dissociation constant (pK_a). The obtained values of pK_{a1} and pK_{a2} are in good agree-

Table 1. The pK_a Values of Ligands C and D at T=310.15 K and I=0.15 $mol\cdot dm^{-3}$ NaCl

System	pK_a±S.D.	Reference
Ligand C		
pK_{a1} (–COOH)	4.39±0.01[a]	4.37[c]
pK_{a2} (*para*-OH)	8.55±0.01[a]	8.55
pK_{a3} (*meta*-OH)	12.46±0.02[b]	12.5
Ligand D		
pK_{a1} (–COOH)	4.55±0.01[a]	4.45[c]
pK_{a2} (*para*-OH)	9.41±0.01[a]	9.43
pK_{a3} (*meta*-OH)	13.65±0.02[b]	13.7

a) Potentiometry technique. *b*) Spectrophotometry technique. *c*) Reference 38, potentiometry, T=298.15 K, I=0.2 $mol\cdot dm^{-3}$ KCl.

ment with those reported in literatures.[26–29,34–37] As shown in Fig. 1, the pK_{a1} of ligands C and D occurs in the carboxylic group, followed by the dissociation of hydroxyl group at the *para*-position (pK_{a2}). This dissociation order is influenced by the inductive properties, π-electron delocalization and polarizability effects.[28]

As the two ligands have similar structure, it is expected that their pK_a values should be similar. However, only pK_{a1} of the ligands showed similar values of 4.39 and 4.55 for ligand C and ligand D, respectively. The pK_{a2} values of ligands C and D (8.55 and 9.41, respectively) are significantly different indicates that the double bond on the carboxylate moiety in ligand C is leading to the electron-withdrawing effect. After losing its first proton on carboxylic group, ligand C has higher ability to rearrange electrons due to electron conjugation system in the structure and proton will be released at lower pH.

The dissociation of hydroxyl group at *meta*-position seems to be affected by dipole effects, leading to the lower acidic property compared to *para*-position. As reported in literatures, pK_{a3} of *meta*-occurred at highly basic pH that is outside the range of reliable measurement by means of potentiometry. Thus, pK_{a3} value was determined by using the spectrophotometry technique. The pK_{a3} obtained for ligand C is 12.46 while for ligand D is 13.65. Evidently from the spectrum of ligand C in Fig. S1(a), at pH 3.0, the ligand possesses three peaks specifically double bands located at 300 and 328 nm (attributed to n–π* bonding) and a single band at 230 nm (attributed to π–π* bonding). The deprotonation from carboxylic group (pH *ca.*

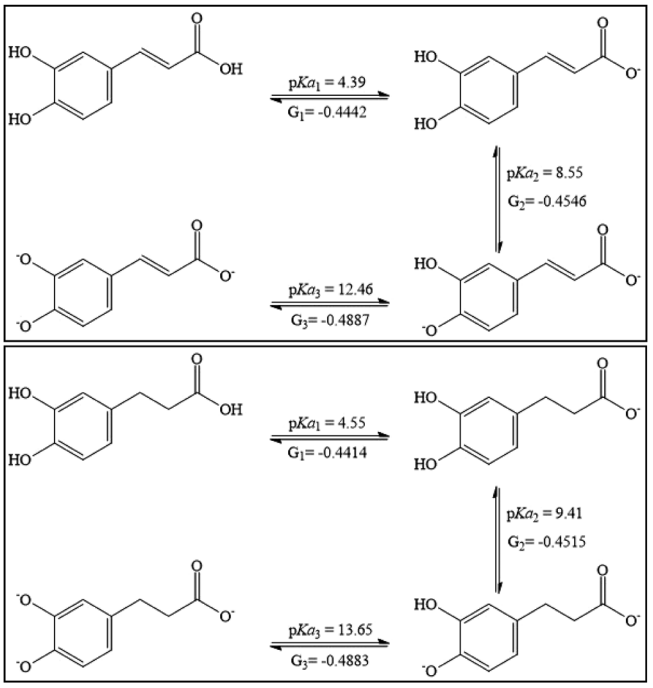

Fig. 1. Proposed Stepwise Dissociation of Ligand C (Top) and Ligand D (Bottom)

Table 2. Logβ of Ligands C and D Binary Complexes at T=310.15 K and I=0.15 mol·dm^{-3} NaCl

Species	Logβ±S.D.[a]					
	Ligand C			Ligand D		
	Pot	Spec	Ref.	Pot	Spec	Ref.
MnL	7.87±0.02	8.13±0.01		9.28±0.02	9.17±0.05	
MnLH	16.03±0.03	—		17.47±0.07	16.00±0.06	
MnL_2	13.8±0.06	—		16.20±0.07	17.97±0.01	
MnL_2H	24.76±0.02 (σ=1.18)[b]	—		27.15±0.02 (σ=1.23)	27.53±0.04	
CoL	8.31±0.01	8.26±0.01		9.56±0.01	9.24±0.02	
CoLH	16.12±0.02	16.09±0.02		17.71±0.02	18.25±0.03	
CoL_2	13.82±0.04	13.76±0.03		16.41±0.04	—	
CoL_2H	24.68±0.02 (σ=1.18)	—		26.59±0.04 (σ=1.24)	—	
NiL	8.85±0.01	8.21±0.02		9.59±0.01	9.31±0.02	
NiLH	15.57±0.04	—		17.48±0.03	17.61±0.02	
NiL_2	13.97±0.02	13.69±0.07		17.52±0.07	16.35±0.03	
NiL_2H	23.3±0.02 (σ=1.17)	23.19±0.02		27.34±0.03 (σ=1.29)	—	
ZnL	9.61±0.01	9.57±0.03		10.58±0.01	10.36±0.01	
ZnLH	15.51±0.02	16.89±0.03		17.72±0.03	—	
ZnL_2	17.47±0.01	17.65±0.04		20.55±0.01	19.96±0.05	
ZnL_2H	25.09±0.05 (σ=1.17)	—		29.71±0.03 (σ=1.24)	—	
CuL	13.14±0.01	13.14±0.02	13.05[c]	13.93±0.03	14.17±0.02	14.1[d]
CuLH	19.00±0.01	19.16±0.02		20.73±0.02	22.09±0.01	
CuL_2	23.32±0.01	23.67±0.03	22.38[c]	25.20±0.03	25.32±0.08	
CuL_2H	29.87±0.05 (σ=1.17)	—		32.86±0.04 (σ=1.17)	—	

a) Logβ obtained from potentiometry−Pot and spectrophotometry−Spec. *b*) Goodness of data fitting in potentiometry measurement. *c*) Reference 28, potentiometry, T=298.15 K, I=0.1 mol·dm^{-3} NaCl. *d*) Reference 38, spectrophotometry, T=298.15 K, I=0.2 mol·dm^{-3} KCl.

5.0) caused a hypsochromic shift of double bands to 292 and 322 nm due to the electron rearrangement along the benzene ring and double bond in the carboxylic moiety. Subsequently, a bathochromic shift at pH *ca.* 9.0 caused by the deprotonated of *para*-hydroxyl group led to the relocation of double band to 302 and 347 nm. Finally, at pH *ca.* 13.0 where the fully deprotonated ligand was formed, the double bands transformed into a single band at 276 nm.

In the case of ligand D in Fig. S1(b), the deprotonation of its carboxyl (pH *ca.* 5.0) group only caused a slight shift in the spectrum. Shift in the spectra started more significantly as the second deprotonation occurred. In the beginning ligand D has two peaks at 210 nm with a shoulder at 227 nm (attributed to π–π^* bonding) and 288 nm (attributed to n–π^* bonding). As pH was gradually increased to 9, the peak at 288 nm disappeared. At pH 13.0, the fully deprotonated ligand was formed and caused bathochromic shift at 220 and 292 nm.

Complex Formation in Binary System Potentiometry and spectrophotometry measurements were used for the determination of complex stability constants ($\log\beta$). The titration curves of ligand C or ligand D binary system at a metal to ligand ratio of 1 : 2.5 are presented in Fig. S2. It is noticeable that as the titrant was added, the metal–ligand curve shifted to lower pH compared to the curve of ligand only indicating the formation of metal complex. The largest shifting was observed in Cu^{2+} system indicated that Cu^{2+} formed the strongest interaction with the ligands.

According to the refinement, various complex species, not only the deprotonated metal–ligand species [ML_n] but also the protonated species [ML_nH_n], were formed. The $\log\beta$ values of binary complexes of ligands C and D are presented in Table 2. It was found that Cu^{2+} formed the most stable complexes with both ligand C and ligand D. Stability constants of metal ions decrease in the following order: $Cu^{2+}>Zn^{2+}>Ni^{2+}>Co^{2+}>Mn^{2+}$, which is also supported by the titration curves. The $\log\beta$ values of ligand C complexes are lower than that of ligand D complexes, which are affected by the electron withdrawing effect of double bond in the carboxylic moiety of ligand C.

Figures 2 and 3 are presented the speciation diagrams for binary systems of ligand C and ligand D, representatively by Cu^{2+} and Zn^{2+}. It is obvious that free metal ion decreased with increasing pH indicating that metal ion formed complex with ligand. In the system involving ligand C, free Cu^{2+} was the earliest to disappear (at pH 6.5) among all the metals indicating that Cu^{2+} exhibited very strong interaction with ligand C. [CuC] species was formed in more acidic pH (4.5) while [ZnC], [NiC], [CoC] and [MnC] started to form at pH 6.0, 6.5, 7.0 and 7.0, respectively. [CuC_2] species was also formed in more acidic pH (6.0) compared to [ZnC_2], [NiC_2],

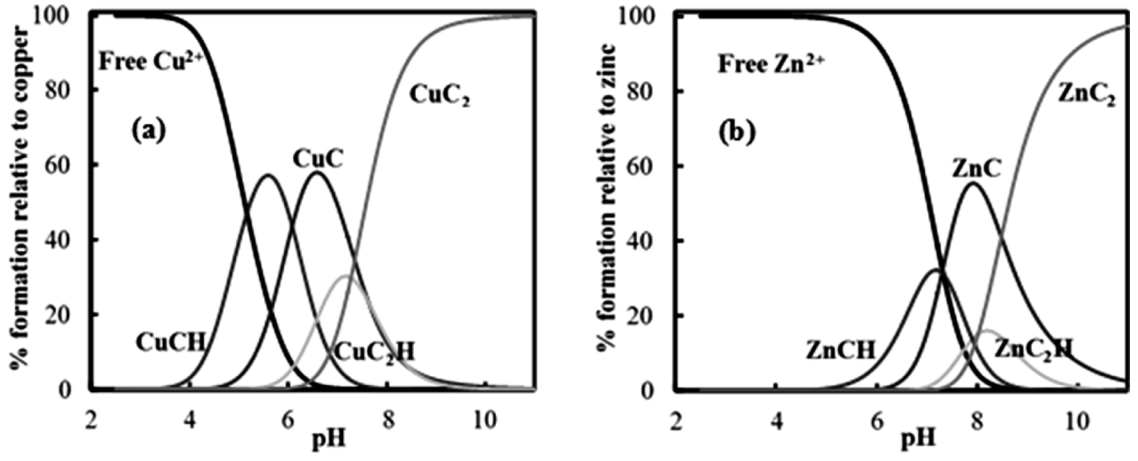

Fig. 2. Speciation Diagram for Binary System of Ligand C with (a) Cu^{2+} and (b) Zn^{2+} at T=310.15 K, I=0.15 mol·dm^{-3} NaCl and [M : L]=1 : 2.5

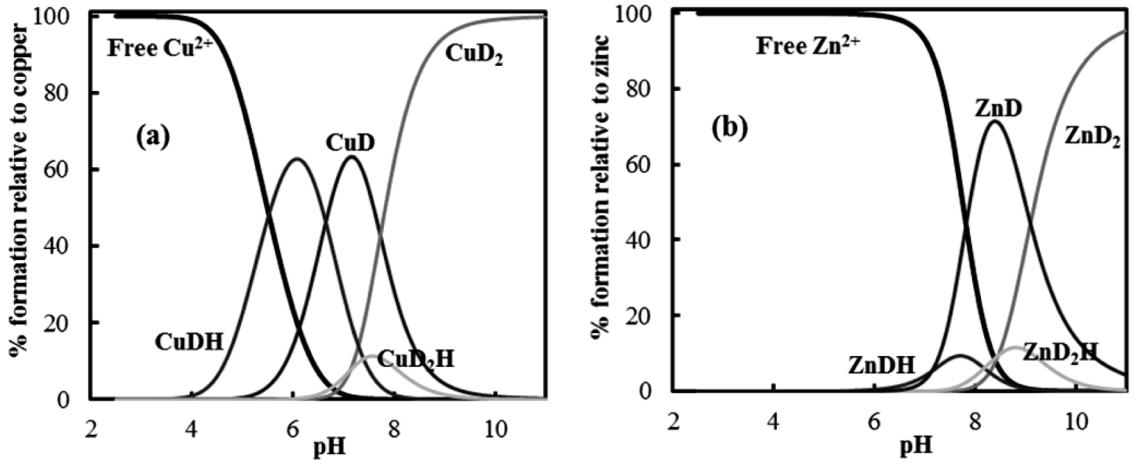

Fig. 3. Speciation Diagram for Binary System of Ligand D with (a) Cu^{2+} and (b) Zn^{2+} at T=310.15 K, I=0.15 mol·dm^{-3} NaCl and [M : L]=1 : 2.5

$[CoC_2]$ and $[MnC_2]$ which was formed pH 7.5, 9.0, 9.0 and 9.5, respectively.

Similar results were also observed in ligand D systems. Cu^{2+} complexes were also started to form at lower pH value compared to other metals. Specifically at pH 5, 6.5, 7.2, 7.4 and 7.5 for [CuD], [ZnD], [NiD], [CoD] and [MnD], respectively; and at pH 6.5, 6.8, 7.3, 7.4 and 7.5 for $[CuD_2]$, $[ZnD_2]$, $[NiD_2]$, $[CoD_2]$ and $[MnD_2]$, respectively.

The protonated complexes [MLH] were the first formed *via* binding with oxygen donor atom of the carboxylic group. The [ML] species began to occur at more basic pH, showing that oxygen donor atom on the catecholate moiety took part in the complex formation. Similarly, $[ML_2H]$ species was also formed at less basic pH than $[ML_2]$ species. The H atom in $[ML_2H]$ species is more likely attributed to the protonated hydroxyl group at *para*-position. While donor atoms that were involved in the formation of $[ML_2]$ species in high basic pH are oxygen atoms on the catecholate moiety. These proposed coordination structures are supported by result of the Gibb's free energy calculation which is discussed in the next section.

Double Bond Effect It was indicated that ligand C has lower pK_as than ligand D. This is because of the presence of unsaturated carbon chain (C double bond) of ligand C which tends to be more reactive than the saturated carbon chain of ligand D. The reactivity of the unsaturated carbon makes the hydrogen atom of ligand C to dissociate faster than ligand D. Evidently from Gibbs free energy (ΔG), dissociation of ligand C is more spontaneous than ligand D where ΔG is more negative. The ΔG values of the dissociation ligand C are $\Delta G_1=-0.4442$, $\Delta G_2=-0.4546$, and $\Delta G_3=-0.4887$, while for ligand D are $\Delta G_1=-0.4414$, $\Delta G_2=-0.4515$, and $\Delta G_3=-0.4883$. Less positive ΔG value indicates more spontaneous reaction.

The effect of bond on stability constant of metal–ligand species was analyzed with Cu^{2+} as the representative metal ion since Cu^{2+} complexes give the most stable species. The ΔG values for Cu^{2+} species with single ligand are summarized in Table 3. Ligand D species exhibit more negative value than ligand C species indicating that ligand D species are more stable. Ligands C and D have similar structure but ligand D species exhibits more negative ΔG value, this phenomenon is because of the double bond effect of ligand C.

The calculation of ΔG can also be used to predict the structure of the species. In Table 3, the proposed model **C** is dedicated for ligand C while model **D** is for ligand D. The proposed structures are presented in Supplementary Fig. S3. [ML] species are indicated by model **C1**, **C2**, **D1** and **D2**, where ΔG for species model **C2** is more negative than **C1**, likewise ΔG for species **D2** is more negative than **D1**. This indicates that between the proposed possible structures, [ML] species are more likely to have the structures as shown by model **C2** and **D2**. Meanwhile for [MLH] species, ΔG for model **C3** is more negative than **C4** and ΔG for **D3** is more negative than **D4**. Thus metal ion in [MLH] species tends to bind *via* carboxyl group of the ligand.

Table 3. Calculated Gibb's Free Energy (ΔG) of Cu^{2+} Species

Model no.	Species	ΔG (Hartree/Particle)
C1	CuC	−0.1456
C2	CuC[a)]	−0.1590
C3	CuCH	−0.1020
C4	CuCH[b)]	−0.0872
D1	CuD	−0.1514
D2	CuD[a)]	−0.1623
D3	CuDH	−0.1078
D4	CuDH[b)]	−0.0931

a) Species with metal ion bond at the two hydroxyl groups or catecholate binding type. *b*) Species with metal ion bond at *para*-hydroxyl group.

Sequestering Ability and Competition Diagram in Binary System Sequestering ability (p$L_{0.5}$) refers to the minimum concentration of a ligand necessary to bind half of the metal available. Since pL is the minus logarithm of ligand concentration, thus a higher pL value implies a smaller ligand concentration. p$L_{0.5}$ values were calculated at the physiological pH (7.4) by the following Eq. (3).

$$X = 1/(1+10)^{(pL-pL_{0.5})} \quad \text{and}$$
$$X = ([M]_{total} - [M]_{free} - \sum [M]_{other})/[M]_{total} \tag{3}$$

where X is the molar fraction of the sum of formation percentages of all metal–ligand species. As can be seen in Table 4, ligand C possesses higher sequestering ability towards Mn^{2+}, Co^{2+} and Cu^{2+} than ligand D. However, in the case of Ni^{2+} and Zn^{2+}, ligand D is more potent than ligand C.

The competition between ligand C and ligand D to bind metal ion was simulated and the results were presented in Fig. 4. It can be observed that ligand C and ligand D compete to bind metal ion. Ligand with stronger binding will result in more dominant species. For instance, in Cu^{2+} system ligand C shows stronger binding and results in more ligand C complex species than that of ligand D. The simulation on the competition between ligand C and ligand D are supported the results on the sequestering ability of the ligands, where at physiological pH ligand C is more potent towards Mn^{2+}, Co^{2+} and Cu^{2+} and ligand D is more potent towards Ni^{2+} and Zn^{2+}. This potentiality can be observed from the percentage of species formed at pH 7.4 shown in Table 5. The percent species formations of Mn^{2+}, Co^{2+} and Cu^{2+} against ligand C are larger than that against ligand D, while for Zn^{2+} and Ni^{2+} their percent species formations against ligand D are larger than that against ligand C as can be seen clearly from species $[ML_2H]$.

In all systems, $[ML_2H]$ species is shown to have the highest percent formation at pH 7.4 except for Cu^{2+} system. For Cu^{2+} system, $[MC_2]$ species started to form at lower basic pH (compare to other metal systems) indicating that Cu^{2+} is the most reactive towards the ligand. This reactivity is also supported by the titration curves (Fig. S2) where Cu^{2+} system exhibits the largest pH shift. The reactivity may trigger the dissociation of the ligand and also the formation of deprotonated species.

Table 4. The p$L_{0.5}$ Values of Ligand C and Ligand D against the Divalent Metal Ions at pH 7.4

Metal ion	p$L_{0.5}$	
	Ligand C	Ligand D
Mn^{2+}	2.66	1.97
Co^{2+}	2.73	2.10
Ni^{2+}	2.73	3.32
Zn^{2+}	3.61	3.95
Cu^{2+}	6.94	5.79

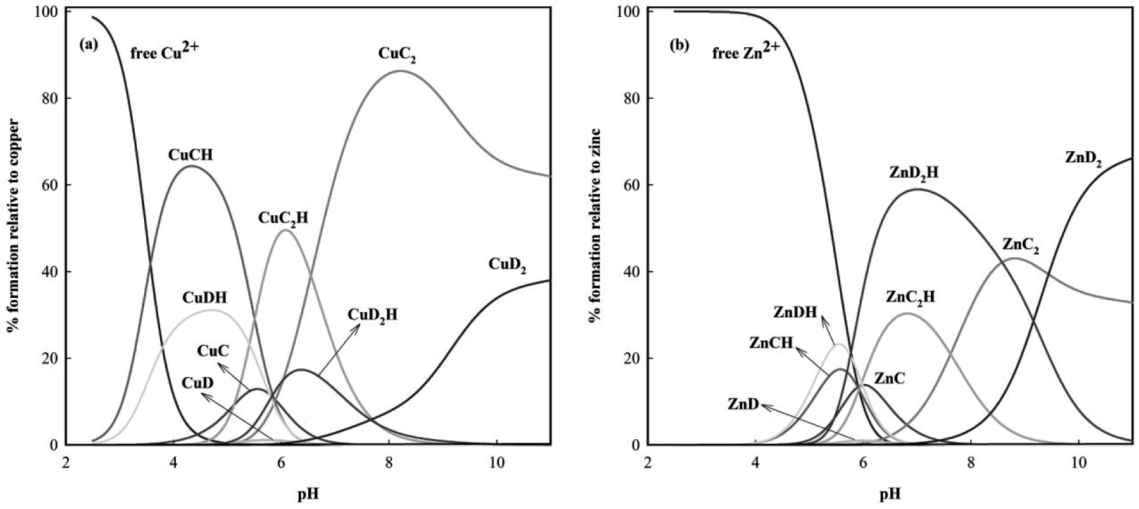

Fig. 4. Competition Diagram for Binary System of Ligands C and D with (a) Cu^{2+} and (b) Zn^{2+}.

Table 5. Percentage of Species Formed in the Competition between Ligands C and D at pH 7.4

M	% Formation relative to M							
	MC	MCH	MC_2	MC_2H	MD	MDH	MD_2	MD_2H
Mn^{2+}	0.29	1.65	0.02	83.20	0.19	1.17	0.004	13.45
Co^{2+}	1.08	2.78	0.03	86.00	0.57	3.23	0.01	6.22
Ni^{2+}	17.36	3.63	0.41	35.31	0.96	2.96	0.15	39.09
Zn^{2+}	1.07	0.03	15.09	25.05	0.07	0.04	1.00	57.65
Cu^{2+}	0.12	0.003	76.29	10.78	0.02	0.01	4.53	8.25

The percentage values were calculated based on logβ from potentiometry data.

Table 6. Logβ of Ternary Complexes in Aqueous Solution at T=310.15 K and I=0.15 mol·dm^{-3} NaCl

Species	Logβ±S.D.[a)]									
	M=Mn^{2+}		M=Co^{2+}		M=Ni^{2+}		M=Zn^{2+}		M=Cu^{2+}	
	Pot	Spec	Pot	Spec	Pot	Spec	Pot	Spec	Pot	Spec
Ligand C										
[MCN]	11.26±0.02	11.30±0.02	11.86±0.05	12.30±0.03	12.56±0.02	12.97±0.08	15.20±0.01	15.55±0.03	17.79±0.03	18.13±0.01
[MCNH]	20.99±0.01	20.74±0.05	21.82±0.03	21.19±0.02	21.93±0.02	21.10±0.03	22.93±0.01	23.41±0.02	26.43±0.03	27.49±0.01
[$MCNH_2$]	—	—	—	—	—	—	—	—	32.60±0.03	—
σ[b)]	1.17		1.24		1.18		1.35		1.17	
Log K^{MC}_{MCN}	3.39	3.17	3.55	3.99	3.71	4.76	5.59	5.98	4.65	4.99
Log K^{MN}_{MCN} [c)]	7.62	—	7.58	—	7.70	—	8.97	—	11.15	—
$\Delta \log K_M$	−0.25		−0.73		−1.15		−0.64		−1.99	
Log X	1.25		1.93		1.93		0.86		−0.44	
Ligand D										
[MDN]	12.02±0.02	12.94±0.06	13.22±0.03	13.11±0.07	13.86±0.02	13.55±0.01	15.72±0.01	15.96±0.01	18.96±0.03	19.07±0.01
[MDNH]	21.66±0.02	22.67±0.01	23.16±0.03	23.62±0.02	23.26±0.02	—	24.03±0.02	24.74±0.01	27.90±0.03	28.35±0.01
[$MDNH_2$]	—	—	—	—	—	—	—	—	34.26±0.04	—
σ[b)]	1.22		1.24		1.21		1.35		1.17	
Log K^{MD}_{MDN}	2.74	3.77	3.66	3.87	4.27	4.24	5.14	5.60	5.03	4.90
Log K^{MN}_{MDN} [c)]	8.38	—	8.94	—	9.00	—	9.49	—	12.32	—
$\Delta \log K_M$	−0.9		−0.62		−0.59		−1.09		−1.61	
Log X	0.37		2.06		1.98		0.22		0.02	

a) Logβ obtained from potentiometry−Pot and spectrophotometry−Spec. *b*) Goodness of potentiometry data fitting using Hyperquad. *c*) Values of $\log\beta_{MN}$ in the determination of $\log K^{MN}_{MCN}$ and $\log K^{MN}_{MDN}$ are 3.64, 4.28, 4.86, 6.23 and 6.64 for M=Mn^{2+}, Co^{2+}, Ni^{2+}, Zn^{2+} and Cu^{2+}, respectively.[22)]

Complex Formation in Ternary System Ternary systems containing ligands C or D and ligand N were studied. The logβ values are presented in Table 6. The stability constant of ternary complexes decreases in the following order of Cu^{2+}>Zn^{2+}>Ni^{2+}>Co^{2+}>Mn^{2+}, where the logβ for [MCN] species are 17.79, 15.2, 12.56, 11.86 and 11.26, while for [MDN] spe-

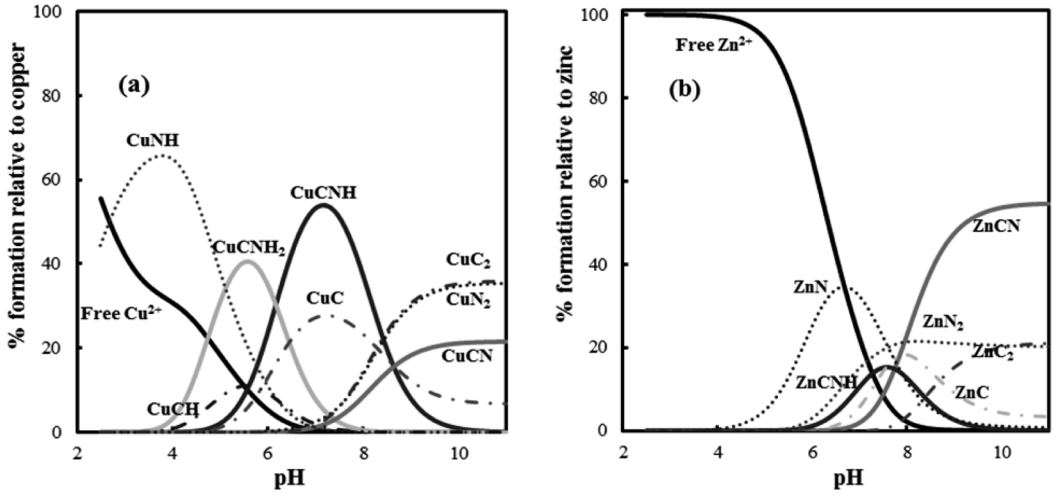

Fig. 5. Speciation Diagram for Ternary System of Ligand C and Ligand N with (a) Cu^{2+} and (b) Zn^{2+} at T=310.15 K and I=0.15 mol·dm^{-3} NaCl

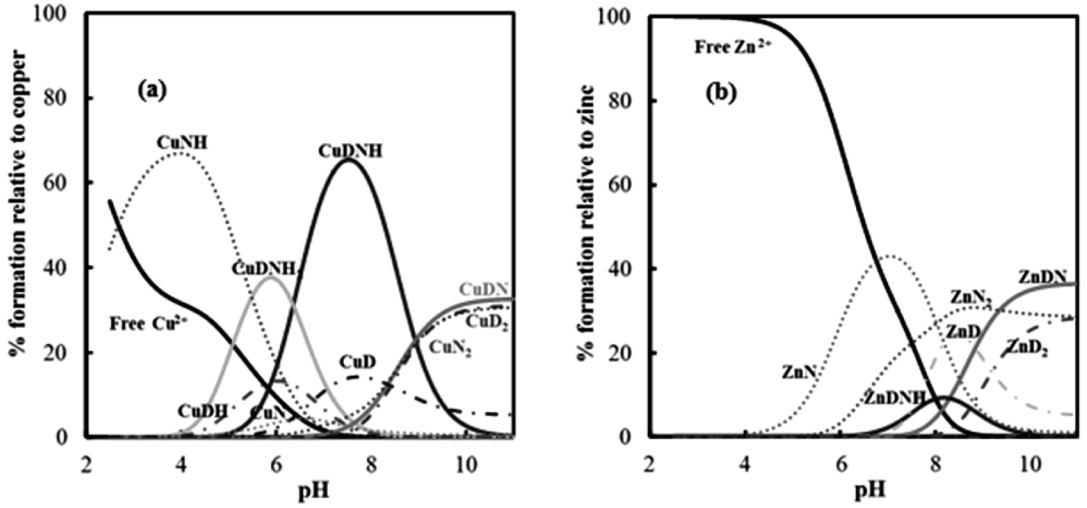

Fig. 6. Speciation Diagram for Ternary System of Ligand D and Ligand N with (a) Cu^{2+} and (b) Zn^{2+} at T=310.15 K and I=0.15 mol·dm^{-3} NaCl

cies are 18.96, 15.72, 13.86, 13.22 and 12.02, for Cu^{2+}, Zn^{2+}, Ni^{2+}, Co^{2+} and Mn^{2+} system, respectively. This trend is also indicated in the titration curves of ternary system (Fig. S4), where the largest shift which indicates the most stable complex is exhibited by Cu^{2+} followed by Zn^{2+}, Ni^{2+}, Co^{2+} and Mn^{2+}. This trend is similar to the binary system. It is also noted that the stability constant values of ligand D system are higher than that of ligand C system. The speciation diagram of ternary systems in Figs. 5 and 6 representatively by Cu^{2+} and Zn^{2+}, indicated that binary species of ligand N formed at lower pH than that of binary species of ligands C and D, thus ligand N was the primary ligand in these systems.

In the formation of [$MLNH_2$] species, the H atoms are originated from *para*- and *meta*-hydroxyl group of ligands C or D, while H atom in [MLNH] species is originated from *meta*-hydroxyl group. The H atoms were not originated from ligand N, since the formation of protonated [MN] species was earlier than protonated [MLH] species. Thus suggested that in the time [$MLNH_2$] and [MLNH] species are formed, all of H atoms of ligand N was already deprotonated. As for [MLN] species, it is formed through the binding of catecholate moiety of either ligands C or D along with carboxyl and thiol groups of ligand N.

Stepwise complexation constant, $\log K^{ML}_{MLN}$ and $\log K^{MN}_{MLN}$, were calculated prior to examining the stability of each single ligand attachment in the formation of ternary complex, the values are shown in Table 6. In all ternary systems $\log K^{ML}_{MLN}$ value is lower than $\log \beta_{MN}$, likewise $\log K^{MN}_{MLN}$ value is lower than $\log \beta_{ML}$. This suggested that attachment of each single ligand in ternary complex is not as stable as in binary complex. Such phenomenon is often encountered by bulky or large molecules. Atoms of a large molecule are close to each other thus induce steric effect between their electron clouds and cause decrease in the stability of the molecule.[39]

The relative stability $\Delta \log K_M$ was employed to explain the tendency of ternary complexes relative to that of binary complexes, which was calculated using Eq. 4.

$$\Delta \log K_M = \log K^{ML}_{MLN} - \log K_{MN} = \log K^{MN}_{MLN} - \log K_{ML} \quad (4)$$

where $\log K^{ML}_{MLN}$ indicated the relative stability of [MLN] over [MN] species and $\log K^{MN}_{MLN}$ indicated the relative stability of [MLN] over [ML] species, L is denoted for ligands C or D. Positive $\Delta \log K_M$ indicates that ternary complex formation is more favorable than that of binary complex. Another parameter to measure the tendency to form either one mole of binary complexes [ML_2] or two moles of ternary complex [MLN] is

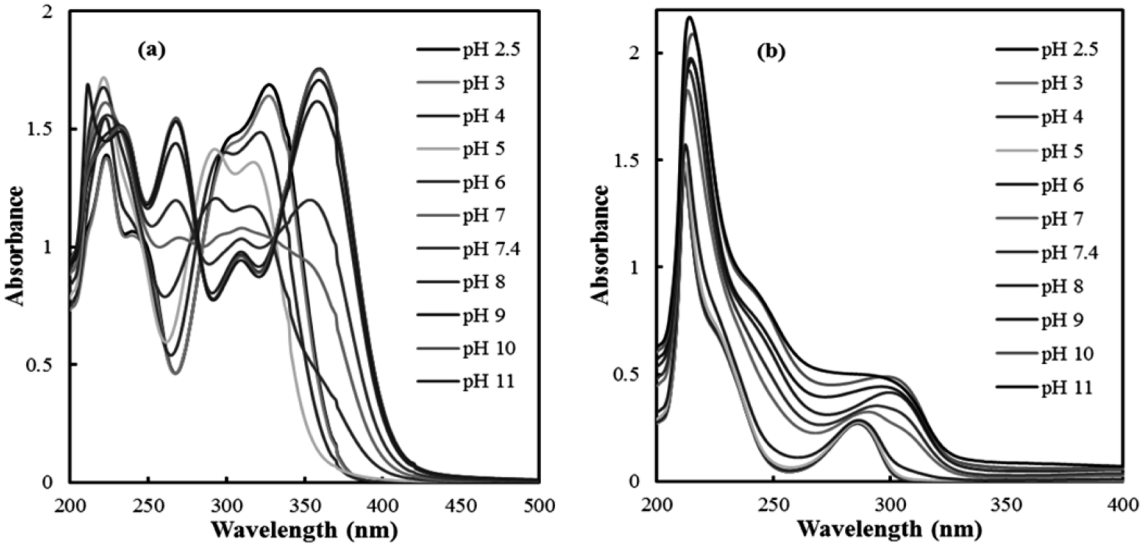

Fig. 7. Spectra of Binary Complex between Cu^{2+} against (a) Ligand C and (b) Ligand D

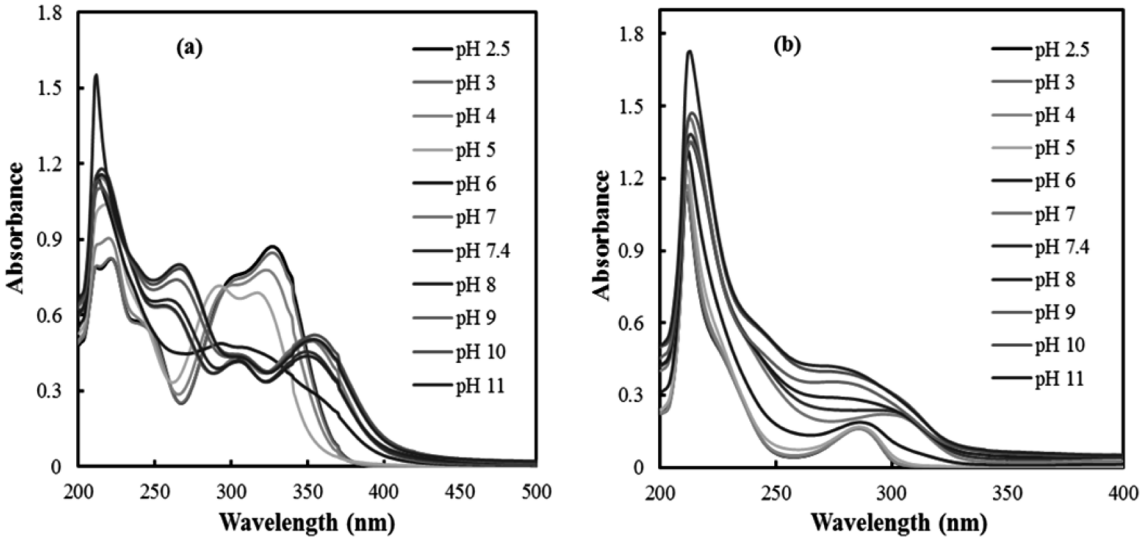

Fig. 8. Spectra of Ternary Complex of Cu^{2+} with (a) Ligand C–N and (b) Ligand D–N

presented as disproportionate constant $\log X$.

$$ML_2 + MN_2 \leftrightarrow 2MLN, \quad X = [MLN]^2 / ([ML_2][MN_2]) \quad (5)$$

$\Delta \log K_M$ and $\log X$ values are shown in Table 6. Generally, $\Delta \log K_M$ indicates the trend opposite to that of stability constant value. Complex with higher stability constant shows more negative $\Delta \log K_M$. It suggests that if a metal ion formed a highly stable binary complex with the first ligand, more energy is needed by the second ligand to participate and form ternary complex. Nevertheless, after ternary complex is formed, it has the stronger stability than that of binary system. Positive value was observed for $\log X$ in almost all systems, suggested that the formation of ternary complex with two different ligands (MCN or MDN) is more favorable than binary complex with two same ligands (MC_2, MD_2 or MN_2). However in the Cu^{2+} system, the $\log X$ was found to be negative which is probably because Cu^{2+} forms a very stable square planar complex with ligand C or D at their catecholate moiety and tends to form complex with two same ligands.

Spectrophotometry Measurement Since the obtained spectra for Mn^{2+}, Co^{2+}, Ni^{2+}, Zn^{2+} and Cu^{2+} are similar for both binary and ternary systems, thus only Cu^{2+} systems were chosen for discussion. From Fig. 7(a) for Cu–C system, it can be seen that in the beginning (pH 2.5) the spectrum for binary complex of ligand C and Cu^{2+} has double bands at 306 and 329 nm, a peak at 228 nm and a shoulder at 247 nm. Based on the speciation diagram, at pH 5 [CuCH] was the dominant species, which led to bathochromic shift of the double bands to 293 and 320 nm, and also caused the disappearance of shoulder at 247 nm. Subsequently, the main species at pH 7 was [CuC], which caused the disappearance of the double bands and the occurrence of a new peak at 270 nm. Then, the species [CuC_2] which was dominant at pH 9 onward, led to a hypsochromic shift of the double bands to 310 and 360 nm. From Fig. 7(b) for Cu–D system, shifting started at pH 6 due to [CuD] species. The formation of this species also caused the disappearance of the shoulder at 227 nm, while the other peaks at 211 and 286 nm did not experience significant changes. At pH 9 onward, the dominant species [CuD_2] initiated the occurrence of two shoulders at 244 and 303 nm.

In Fig. 8(a) for ternary system of Cu–C–N, in the beginning pH of 2.5 the first double band occurred at 209 and 224 nm, the second double band occurred at 306 and 329 nm and a shoulder occurred at 247 nm. As the formation of [$CuCNH_2$] species at pH *ca*. 5, the second double band hypsochromically shifted to 293 and 320 nm and the shoulder band disappeared. Then at pH 10, the formation of [CuCN] species caused a bathochromic shift on the double band to 310 and 359 nm. Similarly for Cu–D–N in Fig. 8(b), at pH 2.5 there are two peaks at 210 and 285 nm with a shoulder at 226 nm. As [CuDNH] was formed at pH 8, the shoulder disappeared and a new peak at 285 nm occurred. Subsequently at pH 10 when [CuDN] species was formed, two new shoulders peak at 245 and 277 nm appears.

Conclusion

The complex equilibrium involving ligand C, ligand D, ligand N and divalent metal ions (Cu^{2+}, Zn^{2+}, Ni^{2+}, Co^{2+}, Mn^{2+}) at T=310.15 K and I=0.15 mol·dm^{-3} NaCl were determined by means of potentiometry and spectrophotometry techniques. The double bond on the carboxylate moiety of ligand C gives electron-withdrawing effect to the system thus the formed complexes is less stable than the complexes of ligand D. This double bond effect also affected the formed ternary complexes where the ternary complexes of ligand C were also less stable than that of ligand D.

In ternary complex, the major factor that influences the stability of the complexes is the steric effect between atoms of the ligands. Since ternary complex is bulkier than binary complex, the steric effect is higher and causes the decrease in stability constant. This effect is indicated by the lower $\log K^{MN}_{MLN}$ compared to $\log\beta_{ML}$, and lower $\log K^{ML}_{MLN}$ compared to $\log\beta_{MN}$. The $\Delta\log K_M$ value of a ternary complex was found to be negative indicating that high energy was needed for ligands to form a ternary complex. The positive value of $\log X$ suggests that the formation of a ternary complex with two different ligands was more favorable than that of a binary complex with two same ligands. Calculated sequestering ability ($pL_{0.5}$) and the competition diagram indicate that ligand C is more potent in binding Mn^{2+}, Co^{2+} and Cu^{2+} while for Ni^{2+} and Zn^{2+} ligand D is found to be more potent.

Acknowledgments This work was supported by the Ministry of Science and Technology of Taiwan (MOST 103-2221-E-011-148) and National Taiwan University of Science and Technology (103B0414).

Conflict of Interest The authors declare no conflict of interest.

Supplementary Materials The online version of this article contains supplementary materials.

References

1) Lansdown A. B. G., "The Carcinogenicity of Metals: Human Risk through Occupational and Environmental Exposure," ed. by Anderson D., Waters M. D., Wilks M. F., Marrs T. C., RSC Publishing, Cambridge, U.K., 2013.
2) Fischwasser K., "Environmental Inorganic Chemistry: Properties, Processes, and Estimation Methods," Vol. 75, ed. by Bodek I., Lyman W. J., Reehl W. F., Rosenblatt D. H., Pergamon Press, New York, 1988.
3) Avila D. S., Luiz R. P., Aschner M., "Interrelations between Essential Metal Ions and Human Diseases," Vol. 13, ed. by Sigel A., Sigel H., Sigel R. K. O., Springer, London, New York, 2013.
4) Nordberg G. F., Fowler B. A., Nordberg M., "Handbook on the Toxicology of Metals," Vol. 1, Elsevier's Science & Technology, Oxford, U.K., 2015.
5) Anderson D., Waters M. D., Marrs T. C., "Issues in Toxicology," ed. by Costa L. G., Aschner M., Royal Society of Chemistry, Cambridge, U.K., 2013.
6) Rink L., "Biomedical and Health Research," Vol. 76, IOS Press, Amsterdam, the Netherlands, 2011.
7) Flora S. J. S., Pachauri V., *Int. J. Environ. Res. Public Health*, **7**, 2745–2788 (2010).
8) Williams D. R., Halstead B. W., *J. Toxicol.*, **19**, 1081–1115 (1982).
9) Andersen O., *Mini Rev. Med. Chem.*, **4**, 11–21 (2004).
10) Taylor D. M., Williams D. R., "Trace element medicine and chelation therapy," Royal Society of Chemistry, Cambridge, U.K., 1995.
11) Rice-Evans C., Miller N., Paganga G., *Trends Plant Sci.*, **2**, 152–159 (1997).
12) Kähkönen M. P., Hopia A. I., Vuorela H. J., Rauha J. P., Pihlaja K., Kujala T. S., Heinonen M., *J. Agric. Food Chem.*, **47**, 3954–3962 (1999).
13) Velioglu Y. S., Mazza G., Gao L., Oomah B. D., *J. Agric. Food Chem.*, **46**, 4113–4117 (1998).
14) Tuan H. M., Ho C. T., Lee C. Y., "Phenolic Compounds in Food and Their Effects on Health II. Antioxidants and Cancer Prevention. In Phenolic Compounds in Food and Their Effects on Health," American Chemical Society, Washington, D.C., U.S.A., 1992.
15) Moon J. H., Terao J., *J. Agric. Food Chem.*, **46**, 5062–5065 (1998).
16) Rajendra Prasad N., Karthikeyan A., Karthikeyan S., Venkata Reddy B., *Mol. Cell. Biochem.*, **349**, 11–19 (2011).
17) Olthof M. R., Hollman P. C., Katan M. B., *J. Nutr.*, **131**, 66–71 (2001).
18) Owen R. W., Haubner R., Mier W., Giacosa A., Hull W. E., Spiegelhalder B., Bartsch H., *Food Chem. Toxicol.*, **41**, 703–717 (2003).
19) Poquet L., Clifford M. N., Williamson G., *Biochem. Pharmacol.*, **75**, 1218–1229 (2008).
20) World Health Organization, "Model List of Essential Medicines," WHO 15, 2007.
21) Pompella A., Visvikis A., Paolicchi A., De Tata V., Casini A. F., *Biochem. Pharmacol.*, **66**, 1499–1503 (2003).
22) Santoso S. P., Chandra I. K., Soetaredjo F. E., Angkawijaya A. E., Ju Y. H., *J. Chem. Eng. Data*, **59**, 1661–1666 (2014).
23) Noszál B., Visky D., Kraszni M. J., *J. Med. Chem.*, **43**, 2176–2182 (2000).
24) Guzeloglu S., Yalcin G., Pekin M. J., *J. Organomet. Chem.*, **568**, 143–147 (1998).
25) Pettit L. D., Powell K. J., Mini S. C., Database, Academic Software: Lexington, KY, 2001.
26) De Stefano C., Lando G., Pettignano A., Sammartano S., *J. Chem. Eng. Data*, **59**, 1970–1983 (2014).
27) Türkel N., Berker M., Ozer U., *Chem. Pharm. Bull.*, **52**, 929–934 (2004).
28) Borges F., Guimaraes C., Lima J. L. F., Pinto I., Reis S., *Talanta*, **66**, 670–673 (2005).
29) Adams M. L., O'Sullivan B., Downard A. J., Powell K. J., *J. Chem. Eng. Data*, **47**, 289–296 (2002).
30) Cornard J. P., Caudron A., Merlin J. C., *Polyhedron*, **25**, 2215–2222 (2006).
31) Gans P., Sabatini A., Vacca A., *Talanta*, **43**, 1739–1753 (1996).
32) Gans P., Sabatini A., Vacca A., *Ann. Chim.*, **89**, 45–49 (1999).
33) Alderighi L., Gans P., Ienco A., Peters D., Sabatini A., Vacca A., *Coord. Chem. Rev.*, **184**, 311–318 (1999).
34) Borges F., Lima J. L. F., Pinto I., Reis S., Siquet C., *Helv. Chim.*, **86**, 3081–3087 (2003).

35) Williams P. A. M., González Baró A. C., Ferrer E. G., *Polyhedron*, **21**, 1979–1984 (2002).
36) Lamy I., Seywert M., Cromer M., Scharff J.-P., *Anal. Chim. Acta*, **176**, 201–212 (1986).
37) Ishimitsu T., Hirose S., Sakurai H., *Talanta*, **24**, 555–560 (1977).
38) Perrin D. D., International Union of Pure, and Applied Chemistry. Commission on Equilibrium Data, "Ionisation Constants of Inorganic Acids and Bases on Aqueous Solution," Pergamon Press, New York, 1982.
39) Chandra I. K., Angkawijaya A. E., Santoso S. P., Ismadji S., Soetaredjo F. E., Ju Y. H., *Polyhedron*, **88**, 29–39 (2015).